

Molecular Cloning of cDNA Encoding a *Drosophila* Ryanodine Receptor and Functional Studies of the Carboxyl-Terminal Calcium Release Channel

Xuehong Xu,* Manjunatha B. Bhat,* Miyuki Nishi,[†] Hiroshi Takeshima,[†] and Jianjie Ma*

*Department of Physiology and Biophysics, Case Western Reserve University School of Medicine, Cleveland, Ohio 44106 USA, and

[†]Department of Pharmacology, University of Tokyo, Tokyo, Japan

ABSTRACT Ryanodine is a plant alkaloid that was originally used as an insecticide. To study the function and regulation of the ryanodine receptor (RyR) from insect cells, we have cloned the entire cDNA sequence of RyR from the fruit fly *Drosophila melanogaster*. The primary sequence of the *Drosophila* RyR contains 5134 amino acids, which shares ~45% identity with RyRs from mammalian cells, with a large cytoplasmic domain at the amino-terminal end and a small transmembrane domain at the carboxyl-terminal end. To characterize the Ca^{2+} release channel activity of the cloned *Drosophila* RyR, we expressed both full-length and a deletion mutant of *Drosophila* RyR lacking amino acids 277–3650 (*Drosophila* RyR-C) in Chinese hamster ovary cells. For subcellular localization of the expressed *Drosophila* RyR and *Drosophila* RyR-C proteins, green fluorescent protein (GFP)-*Drosophila* RyR and GFP-*Drosophila* RyR-C fusion constructs were generated. Confocal microscopic imaging identified GFP-*Drosophila* RyR and GFP-*Drosophila* RyR-C on the endoplasmic reticulum membranes of transfected cells. Upon reconstitution into the lipid bilayer membrane, *Drosophila* RyR-C formed a large conductance cation-selective channel, which was sensitive to modulation by ryanodine. Opening of the *Drosophila* RyR-C channel required the presence of μM concentration of Ca^{2+} in the cytosolic solution, but the channel was insensitive to inhibition by Ca^{2+} at concentrations as high as 20 mM. Our data are consistent with our previous observation with the mammalian RyR that the conduction pore of the calcium release channel resides within the carboxyl-terminal end of the protein and further demonstrate that structural and functional features are essentially shared by mammalian and insect RyRs.

INTRODUCTION

Ryanodine is a neutral alkaloid isolated from the stem woods of the plant *Ryania speciosa* Vahl (Jenden and Fairhurst, 1969). It is a muscle-paralyzing agent that has been used as a botanical insecticide for over 50 years (Pepper and Carruth, 1945; Schmitt et al., 1997). The target site for ryanodine or ryanodine receptor (RyR) is located on the sarcoplasmic reticulum (SR) membrane of muscle cells, where it functions as a Ca^{2+} release channel and mediates the Ca^{2+} release process from the SR membranes in response to excitation of the surface membrane (Fleischer and Inui, 1989; McPherson and Campbell, 1993; Sutko and Airey, 1996). Ryanodine has a biphasic, concentration-dependent effect on the RyR/ Ca^{2+} release channel of mammalian muscles; at nanomolar concentrations it opens the channel or locks it in the open state, and at micromolar concentrations it closes the channel (Meissner, 1984; Witcher et al., 1994). The problem with using ryanodine as an insecticide is that it is toxic to both insects and mammals, and that it can have a muscle-paralyzing effect in humans.

Current research focuses on finding a specific derivative of ryanodine, such as ryanodol or pyridyl ryanodine, with high toxic effects on insects and, at the same time, low toxicity for mammals (Waterhouse et al., 1987; Usherwood and Vais, 1995; Welch et al., 1996, 1997; Bidasee and Besch, 1998). Searching or design of a potent analog of ryanodine with high species specificity would require molecular understanding of the function and regulation of RyR present in the insect cells.

Mammalian cells express three isoforms of RyR, i.e., RyR1, which is mainly present in the skeletal muscle; RyR2 present in the cardiac muscle; and RyR3, referred to as the brain isoform (Takeshima et al., 1989; Otsu et al., 1990; Hakamata et al., 1992). These three isoforms are remarkably similar in primary structure (~66% sequence identity), consisting of ~5000 amino acids (~560 kDa), with a membrane-spanning domain at the carboxyl-terminal end and a hydrophilic domain at the amino-terminal end (Wagenknecht et al., 1989). The carboxyl-terminal domain is predicted to contain 4–12 transmembrane segments, encompassing about one-fifth of the protein size, and forms the putative pore of the Ca^{2+} release channel (Takeshima 1993; Bhat et al., 1997b). The large amino-terminal portion of RyR1 extends into the cytoplasm, presumably contains the binding sites for modulators of the Ca^{2+} release channel, and provides the link with the voltage sensor located in the surface membrane. The binding site(s) for ryanodine, though, is located on the carboxyl-terminal portion of RyR, i.e., within or close to the pore region of the Ca^{2+} release channel (Witcher et al., 1994; Callaway et al., 1994).

Received for publication 30 June 1999 and in final form 10 December 1999.

Address reprint requests to Dr. Jianjie Ma, Department of Physiology and Biophysics, Case Western Reserve University School of Medicine, 10900 Euclid Avenue, Cleveland, OH 44106. Tel.: 216-368-2684; Fax: 216-368-1693; E-mail: jxm63@po.cwru.edu.

Dr. Xu's permanent address is School of Life Sciences, Wuhan University, Wuhan, Hubei 430072, People's Republic of China.

© 2000 by the Biophysical Society

0006-3495/00/03/1270/12 \$2.00

Muscle cells from different insect species also contain abundant amounts of receptor sites for ryanodine (Schmitt et al., 1997; Waterhouse et al., 1987). In *Drosophila*, the ryanodine receptor appears to be expressed during the early stages of embryonic development as well as in the adult tissues of the muscle and nervous systems (Hasan and Rosbash, 1992). Using degenerate cDNA probes from the mammalian isoforms of RyR, Takeshima and colleagues have identified the entire genomic DNA sequence of the *Drosophila* RyR from *D. melanogaster* (Takeshima et al., 1994). Computer analysis predicted that this gene contains 26 exons, comprising the protein-coding sequence for RyR, and the deduced primary amino acid sequence that is ~45% homologous to the mammalian isoforms of RyRs. The carboxyl-terminal portion of *Drosophila* RyR is highly conserved and shows over 90% homology with the corresponding region of mammalian isoforms of RyRs.

To study the function and regulation of the insect Ca^{2+} release channel, we have isolated the complementary DNA sequence coding for *Drosophila* RyR, using a combination of cDNA library screening and reverse transcriptase-polymerase chain reaction (RT-PCR) methods. The complete cDNA has 15,402 base pairs corresponding to the protein-coding sequence of *Drosophila* RyR. The cDNAs encoding the full length or a deletion mutant of *Drosophila* RyR (*Drosophila* RyR-C, lacking a.a. 277-3650) were expressed in Chinese hamster ovary cells. After transient expression, microsomal membrane vesicles were isolated and incorporated into the lipid bilayer membranes for the measurement of single Ca^{2+} release channel activities. Our data show that

the carboxyl-terminal portion of *Drosophila* RyR forms a functional Ca^{2+} release channel with properties similar to those of the Ca^{2+} release channel formed by the carboxyl-terminal portion of the mammalian skeletal muscle RyR (Bhat et al., 1997a,b).

EXPERIMENTAL PROCEDURES

Cloning of *Drosophila melanogaster* ryanodine receptor cDNA

A combination of RT-PCR and cDNA library screening was employed to isolate the entire protein coding cDNA sequence of the *Drosophila* RyR. For RT-PCR, poly(A)⁺ RNA from *Drosophila melanogaster* (Clontech) was used to generate the first- and second-strand cDNA, using the cDNA synthesis kit (Gibco BRL, Gaithersburg, MD) according to the manufacturer's instructions. Based on the availability of the convenient endonuclease restriction sites, five pairs of primers were designed according to the published genomic DNA sequence of the *Drosophila* RyR (Takeshima et al., 1994) (see Table 1). *Sac*II and *Nhe*I restriction sites were included in the PCR I-1F primer for ease of subcloning. In addition, a silent mutation was introduced into the PCR-VF and PCR-IVB primers to change the restriction site for *Nhe*I into one for *Spe*I (GACTAGTC; mutated bases are in boldface) for later subcloning. Using these primers, we generated five PCR fragments (PCR I-1, PCR I-2, PCR II, PCR III, and PCR IV) encoding most of the amino-terminal portion of the *Drosophila* RyR.

TABLE 1 Sequences of PCR primers for *Drosophila* RyR cDNA RT-PCR cloning

Primer name	Sequences	PCR products
PCR I-1F	5'-TCCCGCGGCTAGCCACCATGGCTGAGGCGGAGGGAGG-3'	PCR I-1
	<i>Sac</i> II <i>Nhe</i> I	
PCR I-1B	5'-CGTCCACCACTAGTGTGTTTGGCGACC-3'	PCR I-2
	<i>Spe</i> I	
PCR I-2F	5'-GGTCGCAAAACACTAGTGGTGGAC-3'	PCR I-2
	<i>Spe</i> I	
PCR I-2B	5'-GAAGAACTTAAAGGGGCTGCGG-3'	PCR II
	<i>Not</i> I	
PCR IIF	5'-GATGACAAGAAGAAGCGCGG-3'	PCR II
	<i>Not</i> I	
PCR IIB	5'-TCTTTTCTAGATAGTGTTC-3'	PCR III
	<i>Xba</i> I	
PCR IIIF	5'-ACACTATCTAGAAAAGATCG-3'	PCR III
	<i>Xba</i> I	
PCR IIIB	5'-AACTTGATGTCCCGGTGGC-3'	PCR IV
	<i>Sma</i> I	
PCR IVF	5'-CTTTAAGACGGCCACCGGG-3'	PCR IV
	<i>Sma</i> I	
PCR IVB	5'-ATACTTGGCTAGCCACTTGG-3'	PCR V
	<i>Nhe</i> I	
PCR VF	5'-CGAAGTGACTAGTCAAGTATTTAACACCC-3'	PCR V
	<i>Spe</i> I	
PCR VB	5'-ACGCGTCGACGTTTAAAC TTAGCCGCCGCCCTCCGC-3'	PCR V
	<i>Sal</i> I <i>Pme</i> I	

The cDNA sequence coding for the carboxyl-terminal portion of the *Drosophila* RyR (PCR V) (nt 12,283 to 15,405) was isolated by screening the oligo(dT) and random primed cDNA library for *D. melanogaster* (Clontech). A *XhoI* (12,360)/*EcoRV* (15,027) fragment derived from the genomic clone DRRG-2 (Takeshima et al., 1994) was used as a probe for screening, which yielded nine clones. Detailed restriction analysis revealed that these clones contained cDNA fragments common to the 3' terminal region of the *Drosophila* RyR cDNA. Among the nine overlapping clones, two (λ DRR922 and λ DRR510) were subcloned into pBluescript SK (–) to yield a cDNA fragment from nt 12,283 to nt 15,405. This cDNA fragment was used as a template to generate a PCR product (PCR-V; for primers see Table 1), in which the restriction site for *NheI* (nt 12,283) was changed into a site for *SpeI* (see above).

The cDNA fragments generated by RT-PCR and by cDNA library screening were subcloned into the pBlue-script SK (–) vector and were analyzed by restriction endonuclease digestion and DNA sequencing analysis. PCR I-1 and PCR I-2 were joined together at a *SpeI* site between *SacII* and *NotI* restriction sites to generate PCR I; PCR II and PCR III were joined at a *XbaI* site between *NotI* and *SmaI* sites to generate PCR II-III; PCR IV and PCR V were joined together at *NheI* and *SpeI* sites between *SmaI* and *EcoRI* sites to form PCR IV-V. And PCR I and PCR II-III were ligated together between *SacII* and *SmaI* restriction sites to produce PCR I-III. The full-length *Drosophila* RyR cDNA was finally cloned into the pcDNA 3.1 expression vector (Invitrogen, San Diego, CA) by ligating PCR I-III

and PCR IV-V into pcDNA 3.1 between *NheI* and *EcoRI* restriction sites. All PCR reactions were performed using *Pfu* DNA polymerase (Stratagene, Foster City, CA). The resulting plasmid is named pcDNA3.1 (*Drosophila* RyR).

The sequence of the entire *Drosophila* RyR cDNA was determined using 41 sets of sequencing primers. The differences in the sequence between cloned *Drosophila* RyR cDNA and the published sequence of the *Drosophila* RyR derived from a genomic clone (Takeshima et al., 1994) are listed in Table 2.

Subcloning of *Drosophila* RyR cDNA

The *Drosophila* RyR cDNA contains four restriction sites for *KpnI* (nt 828, 8,700, 9,839, and 10,953), and the pcDNA3.1 vector contains one restriction site for *KpnI* (after the 3' terminal end of the *Drosophila* RyR cDNA). Through digestion of pcDNA3.1 (*Drosophila* RyR) with *KpnI* and religation, an in-frame deletion mutant of *Drosophila* RyR was generated which lacked nucleotides 829 through 10,952. This plasmid is named pcDNA3.1 (*Drosophila* RyR-C). *Drosophila* RyR-C contains 1484 amino acids in the carboxyl-terminal end plus the first 276 amino acids in the amino-terminal end of *Drosophila* RyR.

To identify the subcellular distribution of *Drosophila* RyR expressed in Chinese hamster ovary (CHO) cells, green fluorescent protein (GFP) fusion constructs were generated. First, the GFP-*Drosophila* RyR-C construct was generated by cloning a 4.5-kb *KpnI* (10,953)/*EcoRI*

TABLE 2 Comparison of nucleotide and amino acid sequences deduced from genomic DNA and cloned cDNA of *Drosophila* RyR

Original sequence of Takeshima et al. (1994)	Base pair (site)	<u>AAC</u> (325)	<u>AGC</u> (407)	<u>GAG</u> (679)	<u>GCT</u> (916)	<u>GTC</u> (1041)	<u>ACG</u> (1200)	<u>CTG</u> (3984)	<u>CAG</u> (6093)	<u>CCA</u> (6186)	<u>GAA</u> (7240)	<u>AGT</u> (7646)	<u>CAG</u> (9641)
	Amino acid (site)	<u>N</u> (109)	<u>S</u> (136)	<u>E</u> (227)	<u>A</u> (306)	<u>V</u> (347)	<u>T</u> (400)	<u>L</u> (1328)	<u>Q</u> (2031)	<u>P</u> (2062)	<u>E</u> (2414)	<u>S</u> (2549)	<u>Q</u> (3213)
Cloned sequence of <i>Drosophila</i> RyR cDNA	Base pair (site)	<u>CAC</u> (325)	<u>ACC</u> (407)	<u>AAG</u> (679)	<u>TCT</u> (916)	<u>GTT</u> (1041)	<u>ACA</u> (1200)	<u>CTA</u> (3984)	<u>CAA</u> (6093)	<u>CCG</u> (6186)	<u>CAA</u> (7240)	<u>ATT</u> (7646)	<u>CTG</u> (9641)
	Amino acid (site)	<u>H</u> (109)	<u>T</u> (136)	<u>K</u> (227)	<u>S</u> (306)	<u>V</u> (347)	<u>T</u> (400)	<u>L</u> (1328)	<u>Q</u> (2031)	<u>P</u> (2062)	<u>Q</u> (2414)	<u>I</u> (2549)	<u>L</u> (3213)
Original sequence of Takeshima et al. (1994)	Base pair (site)	<u>GGC</u> (10079)	<u>G₂GT</u> (11969)			<u>AGC</u> (12264)	<u>ATT</u> (12284)	<u>GCT</u> (13131)	<u>TTT</u> (13380)	<u>CCC</u> (13548)	<u>GGC</u> (14094)	<u>GCT</u> (14337)	
	Amino acid (site)	<u>G</u> (3360)	<u>G</u> (3990)			<u>S</u> (4088)	<u>I</u> (4095)	<u>A</u> (4377)	<u>F</u> (4460)	<u>P</u> (4516)	<u>G</u> (4698)	<u>A</u> (4779)	
Cloned sequence of <i>Drosophila</i> RyR cDNA	BASE PAIR (site)	<u>GCC</u> (10079)	<u>GAG TAT ATT CCG</u> (10079)	<u>AGT GCG GGT GCA</u> (11969–11992, 24 base pair insert)		<u>AGT*</u> (12288)	<u>ACT</u> (12308)	<u>GCC</u> (13155)	<u>TTC</u> (13404)	<u>CCG</u> (13572)	<u>GGG</u> (14118)	<u>GCA</u> (14361)	
	Amino acid (site)	<u>A</u> (3360)	<u>E Y I P S A G A</u> (3990– 3997, 8 a.a. insert)			<u>S</u> (4096)	<u>T</u> (4103)	<u>A</u> (4385)	<u>F</u> (4468)	<u>P</u> (4524)	<u>G</u> (4706)	<u>A</u> (4787)	

Silent mutations without amino acid substitutions at 11 positions are found between the sequences derived from a cDNA library and the sequence deduced from the *Drosophila* RyR gene, and thus these mutations are likely due to polymorphism. In contrast, several mutations accompanying amino acid substitutions found between sequences derived from RT-PCR and deduced from the *Drosophila* RyR gene are probably due to errors in PCR. However, the insertion of eight amino acid residues at 3990 represents the correct primary sequence of *Drosophila* RyR because this mutation can be explained by misassignment of intron 22 in the previous report (Takeshima et al., 1994). One of the silent mutations labeled with * was designed for subcloning.

(15,408) fragment encoding the carboxyl-terminal 1484 amino acids of the *Drosophila* RyR behind the 3' terminal end of GFP. Second, the GFP sequence was linked to the 5' terminal end of the full-length *Drosophila* RyR, to generate the GFP-*Drosophila* RyR construct. Both fusion constructs were cloned into the pcDNA3 expression vector (Invitrogen).

Transient expression of *Drosophila* RyR in CHO cells

CHO cells were grown at 37°C and 5% CO₂ in Ham's F-12 medium supplemented with 10% fetal bovine serum, 100 U/ml penicillin, and 100 µg/ml streptomycin. The transfection of cells with the expression plasmids pcDNA3.1 (*Drosophila* RyR-C), pcDNA3.1 (*Drosophila* RyR), pcDNA3 (GFP-*Drosophila* RyR-C), or pcDNA3 (GFP-*Drosophila* RyR) was carried out using LipofectAmine reagent (Gibco) at 60–70% of cell confluence (Bhat et al., 1997a,b). The cells transfected with *Drosophila* RyR-C or GFP-*Drosophila* RyR-C were selected with G418 (0.5 mg/ml) ~48 h after transfection, as in our previous studies (Bhat et al., 1997a–c, 1999). Because of the transient nature of the expression of the full-length *Drosophila* RyR in CHO cells, the cells transfected with *Drosophila* RyR or GFP-*Drosophila* RyR were harvested 24–36 h after transfection.

Western blot of GFP-*Drosophila* RyR and GFP-*Drosophila* RyR-C

CHO cells transfected with pcDNA3(GFP-*Drosophila* RyR) or pcDNA3(GFP-*Drosophila* RyR-C) were harvested and washed twice with ice-cold phosphate-buffered saline and lysed with ice-cold modified RIPA buffer (150 mM NaCl, 50 mM Tris-Cl (pH 8.0), 1 mM EGTA, 1% Triton X-100, 0.1% sodium dodecyl sulfate (SDS), 1% sodium deoxycholate) in the presence of protease inhibitors (Bhat et al., 1997c). The proteins in the whole cell lysate were mixed with the sample buffer (200 mM Tris-Cl (pH 6.7), 9% SDS, 6% β-mercaptoethanol, 15% glycerol, 0.01% bromophenol blue) and separated on a 3–12% gradient SDS-polyacrylamide gel after the samples were heated at 85°C for 5 min. The proteins were then transferred to a polyvinylidene difluoride membrane and blotted with a polyclonal antibody against GFP (Clontech) and horseradish peroxidase-linked secondary antibody, using the enhanced chemiluminescence detection system (Amersham, Arlington Heights, IL).

Confocal imaging of GFP-*Drosophila* RyR-C and GFP-*Drosophila* RyR

CHO cells grown on coverslips were transfected with plasmids for GFP alone (pEGFP-N1, Clontech), pcDNA3(GFP-*Drosophila* RyR-C), or pcDNA3(GFP-*Drosophila* RyR), using the LipofectAmine reagent. Twenty-six hours after transfection, the cells were fixed with 4% paraformaldehyde.

The green fluorescent signals were examined using a Zeiss laser scanning confocal microscope (LSM 410) with a 100× oil immersion objective (Bhat et al., 1997c).

Northern blot analysis

Total RNA was isolated from parental or transfected CHO cells, using the TRIzol reagent (Gibco BRL). RNA (25 µg) of various samples was separated on a 0.8% agarose-formaldehyde gel and transferred onto a GeneScreen Plus membrane (Dupont, Boston, MA). The RNAs were cross-linked by baking the membrane for 30 min at 80°C. A 4.1-kb *KpnI* (10,953)/*EcoRV* (15,024) fragment of *Drosophila* RyR released from pcDNA3.1(*Drosophila* RyR) was used as the cDNA probe, which was radiolabeled with [α -³²P]dCTP, using a Prime-It II random primer labeling kit (Stratagene, Foster City, CA). The RNA on the membrane was hybridized with the probe for 24 h at 42°C in the hybridization solution containing 6× standard saline citrate, 50% formamide, 0.5% SDS, and 5× Denhardt's solution. X-ray film was exposed to the membrane at –70°C and developed 16 h later.

Isolation of microsomal membrane vesicles from CHO cells expressing *Drosophila* RyR

CHO cells expressing *Drosophila* RyR-C or the full-length *Drosophila* RyR were harvested with versene solution (137 mM NaCl, 3 mM KCl, 8 mM Na₂HPO₄, 1.5 mM KH₂PO₄ (pH 7.2), and 0.5 mM EDTA), followed by two washes with ice-cold phosphate-buffered saline. The cell pellet (600 × g, 5 min) was resuspended in ice-cold hypotonic lysis buffer (1 mM EDTA, 5 µM diisopropyl fluorophosphate, 10 µg/ml pepstatin A, 10 µg/ml aprotinin, 10 mg/ml benzamidin, 10 mM HEPES, pH 7.4) and incubated on ice, using nitrogen cavitation (400 pSi for 15 min). After lysis, the cells were homogenized on ice with 10 strokes in a tight-fitting glass Dounce homogenizer, followed by 15 strokes after the addition of an equal volume of restoration buffer (500 mM sucrose, 10 mM HEPES, pH 7.2). Microsomes were collected by centrifugation of postnuclear supernatant (10,000 × g, 15 min) at 100,000 × g for 45 min. The pellet was resuspended in a buffer containing 250 mM sucrose, 10 mM HEPES-Tris (pH 7.2). The membrane vesicles were stored at a protein concentration of 2–6 mg/ml at –70°C until they were used.

Reconstitution of *Drosophila* RyR-C channels in lipid bilayer membrane

Lipid bilayer membranes were formed across an aperture ~200 µm in diameter by the Muller-Rudin method, with a mixture of phosphatidylethanolamine:phosphatidylserine:cholesterol (6:6:1); the lipids were dissolved in decane at a concentration of 40 mg lipid/ml decane (Ma et al., 1994).

Single Ca^{2+} release channels in the bilayer were incorporated by the addition of microsome membranes from cells expressing *Drosophila* RyR-C or *Drosophila* RyR to the *cis*-solution under a concentration gradient of 200 mM Cs-gluconate in *cis*-solution/50 mM Cs-gluconate in *trans*-solution. In experiments to determine the divalent cation selectivity of the *Drosophila* RyR-C channel, Cs-gluconate was replaced with Cs-methane sulfonate (Cs-MES). The free Ca^{2+} concentration in both solutions was buffered with 1 mM EGTA and measured with a Ca^{2+} -sensitive electrode (Orion, Boston, MA).

Single-channel recordings were made with an Axopatch 200A patch-clamp unit (Axon Instruments, Foster City, CA). Data acquisition and pulse generation were performed with an IBM computer and a 1200 Digitdata A/D-D/A converter (Axon Instruments). The offset potential across the bilayer was determined at the end of each experiment, and this value was used to determine the nonconducting baseline and for other data analysis. Single-channel data were analyzed with pClamp7 software, Sigma plot, and custom programs.

RESULTS

cDNA construction of the *Drosophila* ryanodine receptor

RT-PCR and cDNA library screening were used to amplify the entire coding sequence of the *Drosophila* ryanodine receptor (*Drosophila* RyR) cDNA from *D. melanogaster*. Using forward and backward primers based on the published genomic DNA sequence of *Drosophila* RyR (Table

1), we obtained and sequenced six overlapping cDNA fragments (Fig. 1). The entire protein-coding sequence of the *Drosophila* RyR cDNA contains 15,405 base pairs, with a deduced amino acid sequence identical to that predicted by the genomic DNA sequence reported by Takeshima et al. (1994), except for one major difference: the identified cDNA clone contains 24 extra base pairs that are inserted after nucleotide position 11,968 (in PCR IV), $\text{G}_{\text{ins}}^{\text{A}^{11,969}} \text{G TAT ATT CCG AGT GCG GGT GCA G}^{11,992} \text{GT}$, which lead to the insertion of extra eight amino acids near the carboxyl-terminal portion of *Drosophila* RyR, $\text{E}^{3990} \text{YIPSA GA}^{3997}$ (Table 2). Twelve additional silent mutations and eight missense mutations involving changes in single base pairs were identified, which are probably errors caused by the PCR procedure. One of the 12 silent mutations, $\text{AGC} \rightarrow \text{AGT}^{12,288}$, was intentionally designed to replace the restriction site for *NheI* with that of *SpeI* for later subcloning (see Experimental Procedures).

These six PCR products were subcloned into the pBlue-script SK(-) vector and were subsequently linked together in four ligation steps to produce PCR I-III and PCR IV-V (Fig. 1). The final plasmid containing the complete *Drosophila* RyR cDNA sequence was obtained by joining PCR I-III and PCR IV-V into the pcDNA3.1 expression vector.

Expression and subcellular localization of *Drosophila* RyR in CHO cells

For structure-function studies of the *Drosophila* RyR channel, three additional expression plasmids were generated. First, a deletion mutant of *Drosophila* RyR was obtained

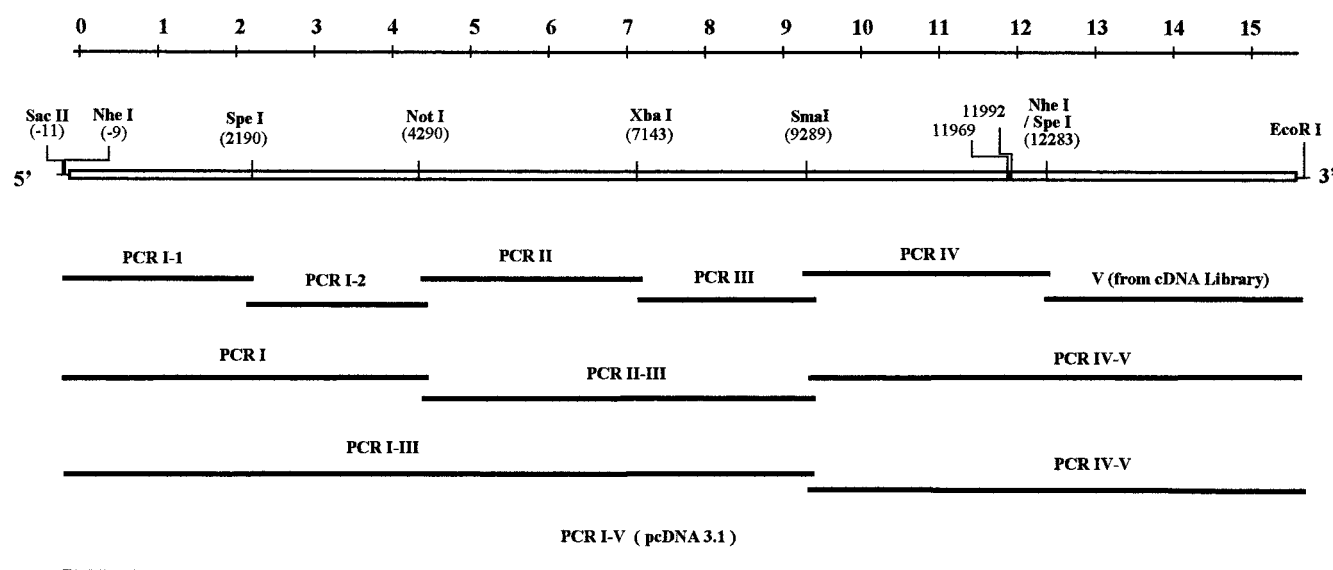


FIGURE 1 RT-PCR cloning of the *Drosophila* ryanodine receptor cDNA. Six PCR products were generated using forward and backward primers designed according to the published genomic DNA sequence of *Drosophila* RyR (Takeshima et al., 1994). These products were subcloned into pBlue-script SK(-) vector and joined together in four ligation reactions to generate PCR I-III and PCR IV-V. The cDNA fragment carrying the entire sequence of *Drosophila* RyR was cloned into the pcDNA3.1 expression vector by ligating PCR I-III and PCR IV-V into the *NheI* and *EcoRI* restriction sites.

through digestion of pcDNA3.1(*Drosophila* RyR) with *Kpn*I (see Experimental Procedures). This mutant lacks amino acids 277-3650 and encodes mostly the transmembrane domain of *Drosophila* RyR at the carboxyl-terminal end, and thus is named *Drosophila* RyR-C. Second, the cDNA sequence for GFP was attached to the 5' end of *Drosophila* RyR-C; the resulting construct is named GFP-*Drosophila* RyR-C. Third, the GFP sequence was ligated to the 5' end of the full-length *Drosophila* RyR to obtain the GFP-*Drosophila* RyR fusion construct.

The plasmids encoding GFP-*Drosophila* RyR-C and GFP-*Drosophila* RyR were introduced into the CHO cells with the LipofectAmine reagent (Bhat et al., 1997b, 1997c). For positive controls, CHO cells were transfected with pEGFP-N1 that encodes only GFP. Twenty-six hours after transfection, the CHO cells expressing GFP, GFP-*Drosophila* RyR-C, or GFP-*Drosophila* RyR were visualized under a confocal microscope for subcellular localization of expressed proteins in these cells. As shown in Fig. 2 *A*, CHO cells expressing GFP alone exhibit a diffuse pattern of green fluorescence as expected for a soluble protein, whereas cells expressing GFP-*Drosophila* RyR-C and GFP-*Drosophila* RyR exhibited fluorescence signals only in certain subcellular areas (Fig. 2, *B* and *C*), particularly in the perinuclear region, indicating that the protein is probably localized in the endoplasmic reticulum (ER) membrane of CHO cells.

To confirm the expression of *Drosophila* RyR in CHO cells, Northern blot analysis was carried out using total RNA isolated from the parental CHO cells and from cells transfected with cDNA for *Drosophila* RyR, *Drosophila* RyR-C, or GFP-*Drosophila* RyR-C, separately. The mRNA-cDNA hybridization revealed a single band of ~5.3 kb and ~5.2 kb in CHO cells transfected with *Drosophila* RyR-C and GFP-*Drosophila* RyR-C, respectively, and a band of ~15.6 kb in cells transfected with *Drosophila* RyR (Fig. 3 *A*). These sizes are as expected for the mRNA of *Drosophila* RyR-C (4.5-kb C-terminal cDNA plus 0.8-kb N-terminal cDNA; Fig. 3 *A*, lane 2), GFP-*Drosophila* RyR-C (4.5-kb C-terminal cDNA plus 0.7-kb GFP coding sequence; Fig. 3 *A*, lane 3), and *Drosophila* RyR (15.6-kb

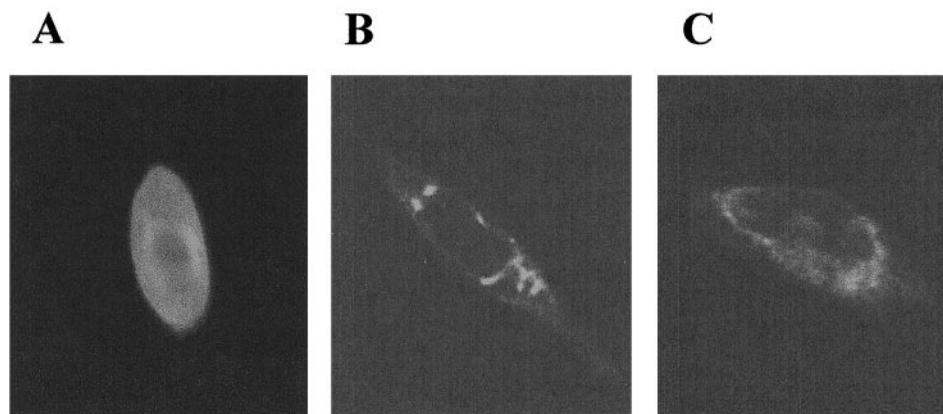
cDNA). The parental CHO cells contain no detectable transcripts of *Drosophila* RyR (Fig. 3 *A*, lane 1).

The expression of *Drosophila* RyR in CHO cells was further examined by Western blot analysis. Because of the lack of specific antibodies against the *Drosophila* RyR protein, we used the GFP-*Drosophila* RyR and GFP-*Drosophila* RyR-C fusion constructs, which allowed us to use antibody against GFP for the detection of expressed proteins. As shown in Fig. 3 *B*, 24 h after transfection of the CHO cells with GFP-*Drosophila* RyR or GFP-*Drosophila* RyR-C, a protein band of ~590 kDa was observed with GFP-*Drosophila* RyR, and ~190 kDa was observed with GFP-*Drosophila* RyR-C. The cells transfected with GFP alone exhibited a protein band of ~26 kDa. Notice that the level of protein expression with the full-length *Drosophila* RyR is significantly lower than that with the carboxyl-terminal portion of *Drosophila* RyR. And furthermore, continued growth of the cells beyond 72 h resulted in complete loss of *Drosophila* RyR protein expression ($n = 6$, not shown). This is likely due to a certain toxic effect(s) of the insect RyR on the CHO cells, inasmuch as stable expression of the mammalian isoforms of RyRs (skeletal and cardiac RyRs) has been achieved in HEK 293 cells (Gao et al., 1997; Wayne Chen et al., 1997; Du et al., 1998) and in CHO cells in our previous studies (Bhat et al., 1997b,c, 1999).

Single-channel measurement with the full-length *Drosophila* RyR

The CHO cells expressing the full-length *Drosophila* RyR proteins were harvested 24–36 h posttransfection, and microsomal membrane vesicles were prepared following the procedure of Bhat et al. (1997a). These vesicles were fused with the lipid bilayer membrane for measurement of single-channel activities formed by the *Drosophila* RyR proteins. To facilitate identification of the Ca^{2+} release channels, 200 mM Cs-gluconate was used in the recording solution. The use of Cs as the current carrier allows for buffering of free $[\text{Ca}^{2+}]$ to any desired level. In addition, Cs eliminates the K

FIGURE 2 Confocal imaging of GFP-*Drosophila* RyR expressed in CHO cells. Confocal imaging of a single CHO cell expressing GFP alone (*A*), GFP-*Drosophila* RyR-C fusion protein (*B*), or GFP-*Drosophila* RyR fusion protein (*C*). GFP exhibits a diffuse pattern of fluorescence, and the signals for both GFP-*Drosophila* RyR-C and GFP-*Drosophila* RyR are localized to the perinuclear region. The pictures were taken ~26 h after transfection of the corresponding plasmids into the CHO cells.



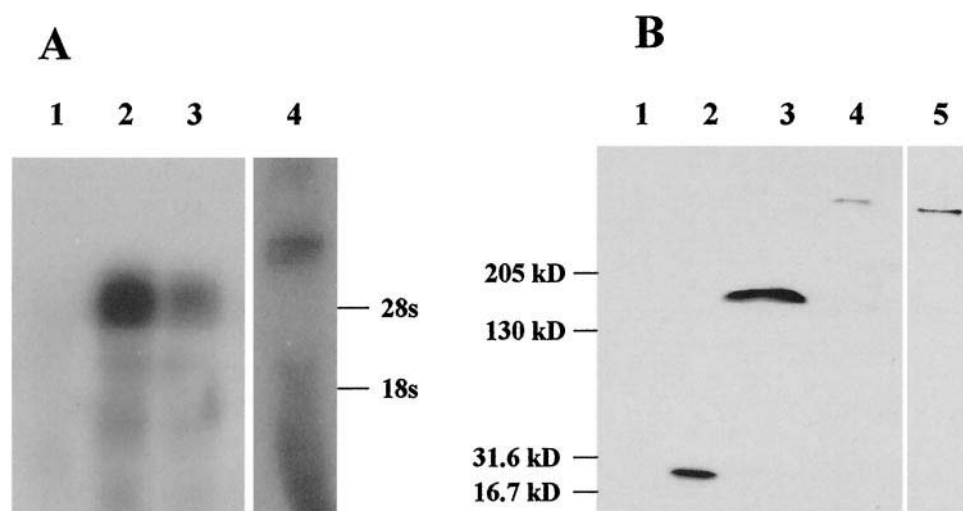


FIGURE 3 Transient expression of *Drosophila* RyR in CHO cells. (A) Northern blot of CHO cells transfected with *Drosophila* RyR-C (lane 2), GFP-*Drosophila* RyR-C (lane 3), or the full-length *Drosophila* RyR (lane 4). Lane 1: Parental CHO cells. (B) Western blot of GFP-*Drosophila* RyR and GFP-*Drosophila* RyR-C transiently expressed in CHO cells. CHO cells were harvested ~24 h after transfection with pcDNA3(GFP-*Drosophila* RyR) or pcDNA3(GFP-*Drosophila* RyR-C). The cells were lysed with the RIPA buffer, loaded onto a 3–12% gradient SDS-polyacrylamide gel, and blotted with a polyclonal antibody against GFP. Lane 1: Parental CHO cells; lane 2: cells transfected with GFP; lane 3: cells transfected with GFP-*Drosophila* RyR-C; lane 4: cells transfected with GFP-*Drosophila* RyR. Lane 5 contains proteins from CHO cells stably expressing the mammalian skeletal RyR, and was blotted with a monoclonal antibody against RyR1.

channel activities that are present in the ER membranes of CHO cells. The large anion gluconate does not permeate through the Cl channels in the microsomal membrane vesicles.

Fig. 4 shows representative single-channel current traces of the full-length *Drosophila* RyR with 26 μ M free $[Ca^{2+}]$ present in the *cis*-cytoplasmic solution. The channel has fast kinetics of gating, with fast transitions between the open and closed states (Fig. 4 A), which are similar to those of the rabbit skeletal muscle Ca^{2+} release channel expressed in CHO cells (Bhat et al., 1997b). A characteristic feature of the *Drosophila* RyR channel is the frequent appearance of a

subconductance state that seems to be linked to the full open state of the channel (see also Fig. 5). With 200 mM Cs-gluconate as the current carrier, the *Drosophila* RyR channel exhibits a linear current-voltage relationship, with a slope conductance of 507 ± 10 pS (Fig. 4 B). This conductance value is significantly larger than that for the rabbit skeletal and cardiac Ca^{2+} release channels expressed in CHO cells (Bhat et al., 1997b,c). Compared with the *Drosophila* RyR-C channel (see below), a detailed biophysical characterization of the full-length *Drosophila* RyR channel was difficult because of the low-level and transient nature of

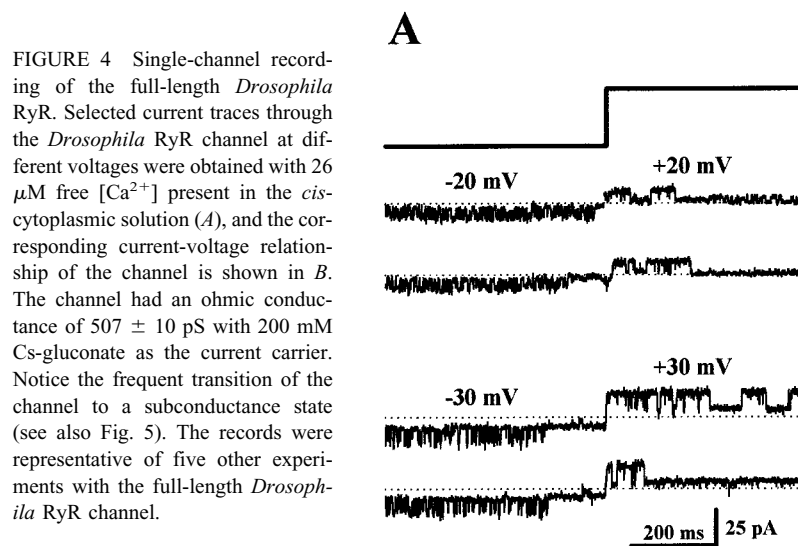


FIGURE 4 Single-channel recording of the full-length *Drosophila* RyR. Selected current traces through the *Drosophila* RyR channel at different voltages were obtained with 26 μ M free $[Ca^{2+}]$ present in the *cis*-cytoplasmic solution (A), and the corresponding current-voltage relationship of the channel is shown in B. The channel had an ohmic conductance of 507 ± 10 pS with 200 mM Cs-gluconate as the current carrier. Notice the frequent transition of the channel to a subconductance state (see also Fig. 5). The records were representative of five other experiments with the full-length *Drosophila* RyR channel.

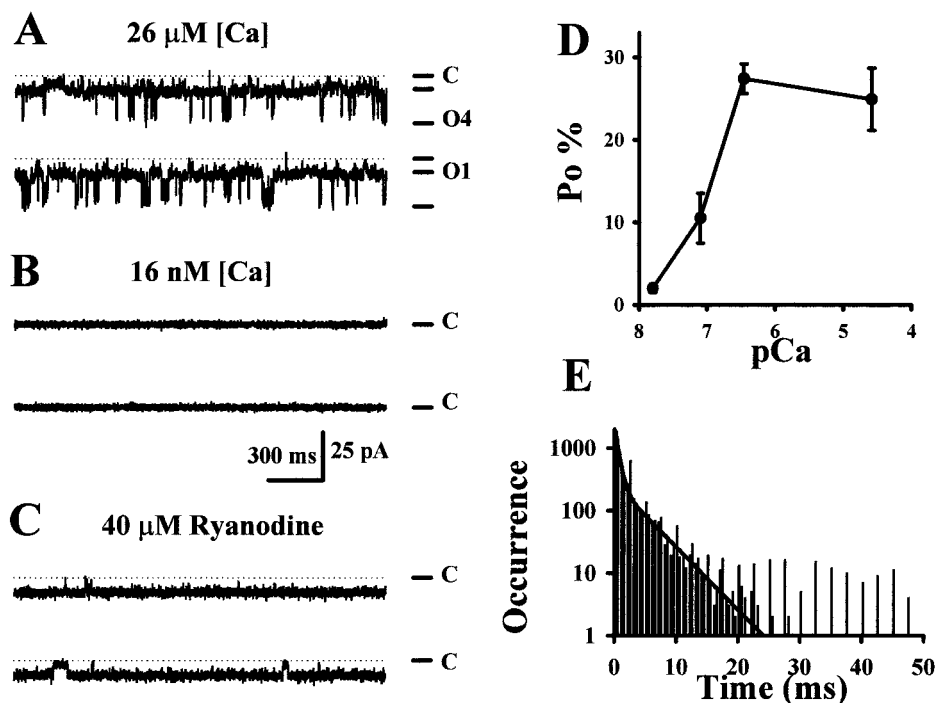


FIGURE 5 Single-channel measurements of the *Drosophila* RyR-C channel: representative current traces through the *Drosophila* RyR-C channel with 26 μM free $[\text{Ca}^{2+}]$ present in the *cis*-cytoplasmic solution (A), after the addition of 20 mM EGTA to the *cis* solution, which chelates the free $[\text{Ca}^{2+}]$ to 16 nM and results in complete inhibition of the channel (B). O4 represents the full conductance state ($i = -25$ pA), and O1 is the subconductance state ($i = -7$ pA) of the channel. Ryanodine (40 μM) added to both *cis* and *trans* solutions reduced single-channel conductance by $\sim 50\%$ and increased the channel open probability by over 20-fold (C). (D) Dose-dependent activation of the *Drosophila* RyR-C channel by the cytoplasmic Ca^{2+} . The data points represent mean \pm SEM ($n = 4$). (E) The open time histogram of the *Drosophila* RyR-C channel at -50 mV was generated with data obtained from eight separate experiments at 26 μM free $[\text{Ca}^{2+}]$. The total number of open events is 4498. The solid line represents the fit according to $y = y_{01}/\tau_{01} \exp(-t/\tau_{01}) + y_{02}/\tau_{02} \exp(-t/\tau_{02})$, where y_{01} and y_{02} represent the proportion of the channel spent in the τ_{01} and τ_{02} states, respectively. The best fit parameters are $y_{01} = 0.538$, $\tau_{01} = 0.591$ ms and $y_{02} = 0.462$, $\tau_{02} = 4.33$ ms.

protein expression in CHO cells. Thus the present study focused on the functional characterization of the Ca^{2+} release channel formed by the carboxyl-terminal portion of *Drosophila* RyR.

Single-channel recording of *Drosophila* RyR-C

CHO cells expressing the *Drosophila* RyR-C proteins were cultured in a selection media containing G418. Approximately 5–7 days later, when the cells reached $\sim 95\%$ confluence, the cells were harvested and microsomal membrane vesicles were isolated for the reconstitution studies, using the lipid bilayer system. Fig. 5 A shows representative single-channel current traces of *Drosophila* RyR-C with 26 μM free $[\text{Ca}^{2+}]$ present in the *cis*-cytoplasmic solution. The channel has fast kinetics of gating, with average open lifetimes of 0.59 ms and 4.33 ms (Fig. 5 E). Similar to the full-length *Drosophila* RyR channel, the *Drosophila* RyR-C channel also exhibited frequent transitions to a subconductance state (O1), which appears to be linked to the full open state of the channel (O4). At -50 mV, the O1 state has a single-channel current amplitude of -7.80 ± 0.41 pA ($n = 9$), which is approximately one-fourth that of the O4 state

(-27.63 ± 1.10 pA, $n = 9$). This unique subconductance state of the *Drosophila* RyR channel is likely due neither to degradation of the *Drosophila* RyR proteins nor to incorporation of multiple channels into the bilayer membrane, based on the following studies. First, similar subconductance states were observed in both the *Drosophila* RyR and *Drosophila* RyR-C channels (see Figs. 4 A and 5 A); second, both full- and subconductance states were sensitive to inhibition by EGTA (see Fig. 5 B). Furthermore, we have comparative studies with the mammalian RyR channels expressed in CHO cells. With experiments conducted under identical conditions (same protocol of gene transfection, vesicle isolation, bilayer reconstitution), the close connection between the full- and subconductance states seen in the *Drosophila* RyR channel was rarely observed with the skeletal and cardiac RyR channels expressed in the CHO cells (Bhat et al., 1997b, 1999). These data argue against the possibility that the subconductance states represent a different channel (or multiple channels) incorporated into the bilayer membrane.

Opening of the *Drosophila* RyR-C channel requires the presence of micromolar concentration of Ca^{2+} in the *cis*-cytoplasmic solution, as the addition of 20 mM EGTA,

which chelates the free $[Ca^{2+}]$ to 16 nM, results in complete closure of the *Drosophila* RyR-C channel (Fig. 5 B). Half-activation of the *Drosophila* RyR-C channel requires the presence of $\sim 0.2 \mu M$ $[Ca^{2+}]$ in the myoplasmic solution (Fig. 5 D). The *Drosophila* RyR-C channel also retains its sensitivity to modulation by ryanodine, as the addition of 40 μM ryanodine results in significant changes in the gating properties of the *Drosophila* RyR-C channel. The ryanodine-modified *Drosophila* RyR-C exhibited a single-channel conductance that was $\sim 30\%$ of the full conductance state, and the open lifetime of the channel was increased by over 20-fold (Fig. 5 C). With vesicles isolated from untransfected CHO cells, these typical large-conductance ryanodine-sensitive channels were never observed (Bhat et al., 1997b).

Fig. 6 shows the effect of increasing concentrations of cytosolic $[Ca^{2+}]$ on the *Drosophila* RyR-C channel. With 26 μM free $[Ca^{2+}]$ present in the *cis*-solution, the *Drosophila* RyR-C channel had an average open probability (P_o) of $24.9 \pm 6.8\%$ ($n = 12$) at -50 mV (Fig. 6, A and C). Increasing the free $[Ca^{2+}]$ to millimolar concentrations did not result in significant changes in the P_o of the *Drosophila* RyR-C channel. The traces shown in Fig. 6 B were obtained with 20 mM free $[Ca^{2+}]$ present in the *cis* solution. Under this condition, the channel had an average P_o of $27.0 \pm 3.5\%$ (Fig. 6 C, $n = 8$). This is in contrast to the Ca^{2+} -dependent inactivation observed with the full-length mammalian RyR1 channel expressed in CHO cells (Bhat et al., 1997a,b). Thus the *Drosophila* RyR-C channel lacks apparent Ca^{2+} -dependent inactivation.

These properties of the *Drosophila* RyR-C channel are similar to those of the Ca^{2+} release channel formed by the carboxyl-terminal portion of RyR1 from rabbit skeletal muscle (RyR-C) (Bhat et al., 1997b). Both *Drosophila* RyR-C and mammalian skeletal muscle RyR-C lack a large portion of the cytoplasmic domain of the ryanodine receptor (a.a. 277-3650 in *Drosophila* RyR and a.a. 183-4006 in mammalian RyR1), and both of them are capable of forming functional Ca^{2+} release channels that are sensitive to acti-

vation by cytosolic Ca^{2+} and to modulation by ryanodine. In addition, both *Drosophila* RyR-C and mammalian RyR-C channels appear to lack the Ca^{2+} -dependent inactivation mechanism.

Comparison of the *Drosophila* RyR-C channel with the RyR-C channel from mammalian cells

In our previous studies with the mammalian RyR1 expressed in CHO cells, we showed that the RyR-C channel exhibited inward rectification in its current-voltage relationship (Bhat et al., 1997b). With 200 mM symmetrical Cs-gluconate as the current carrier, the RyR-C channel had a linear conductance of 407 pS in the negative voltage range (Cs ions moving from SR lumen to cytosol) and a linear conductance of 332 pS in the positive voltage range (Cs ions moving from cytosol to SR lumen) (see Fig. 7 C). This inward-rectification behavior was also observed with the *Drosophila* RyR-C channel under identical recording conditions, but the *Drosophila* RyR-C channel differs significantly from the mammalian RyR-C channel in terms of single-channel conductance. The single-channel traces shown in Fig. 7 A were taken from a *Drosophila* RyR-C channel, and the traces shown in Fig. 7 B were taken from a mammalian RyR-C channel, under identical experimental conditions. Both inward and outward currents through the *Drosophila* RyR-C channel were significantly larger than those through the RyR-C channel. At -50 mV, the *Drosophila* RyR-C channel had a single-channel current $i = -27.63 \pm 1.10$ pA, whereas the corresponding value for the RyR-C channel was $i = -20.24 \pm 0.69$ pA (Bhat et al., 1997b). The complete I - V relationship of the mammalian and *Drosophila* RyR-C channels is shown in Fig. 7 C. Here, the *Drosophila* RyR-C channel had an inward conductance of 553 pS and an outward conductance of 442 pS, which are $\sim 35\%$ larger than the corresponding values for the RyR-C channel (Bhat et al., 1997b). The inward conductance of the *Drosophila* RyR-C channel is similar to that of the full-length *Drosophila* RyR channel (Fig. 4).

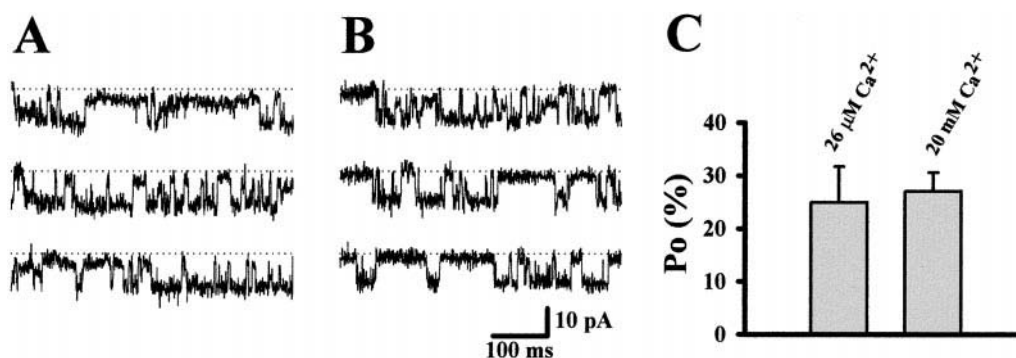


FIGURE 6 Ca^{2+} -dependent regulation of the *Drosophila* RyR-C channel: selected single-channel current traces from the same experiment, with 26 μM free $[Ca^{2+}]$ (A) or 20 mM free $[Ca^{2+}]$ (B) present in the *cis* solution. (C) The average open probabilities (P_o) of the *Drosophila* RyR-C channel were calculated from multiple experiments at two different concentrations of $[Ca^{2+}]$. The data represent mean \pm SEM.

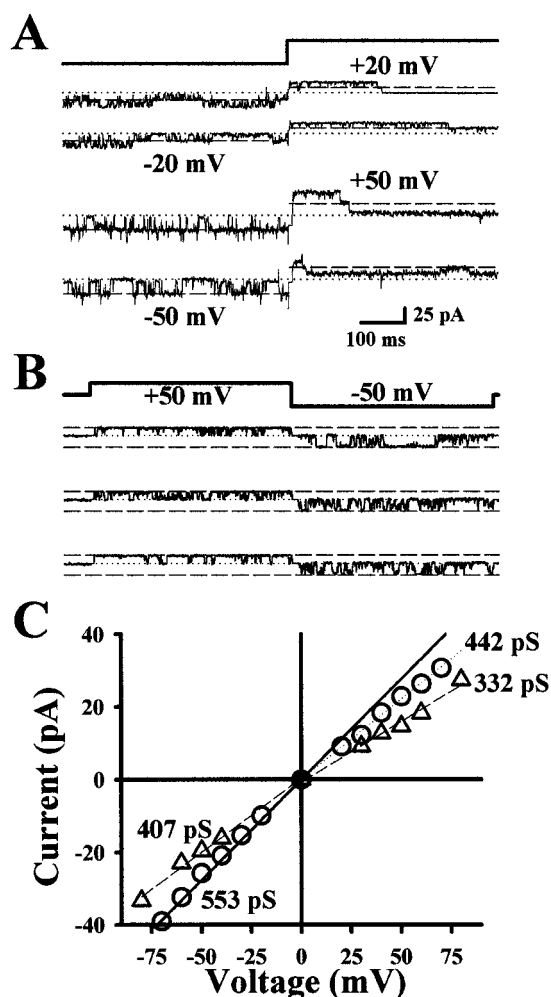


FIGURE 7 Comparison of *Drosophila* RyR-C with mammalian RyR-C and I-V relationship of *Drosophila* RyR-C channel. (A) Selected current traces from the *Drosophila* RyR-C channel acquired with a test pulse from -20 mV to $+20$ mV and from -50 mV to $+50$ mV, with 200 mM Cs-gluconate as the current carrier. (B) Representative current traces from the mammalian RyR-C channel at $+50$ mV and -50 mV, under experimental conditions identical to those in A. RyR-C is a deletion mutant of RyR from rabbit skeletal muscle, which lacks amino acids 183-4006 in the cytosolic domain of mammalian RyR1 (Bhat et al., 1997b). (C) Current-voltage relationship of *Drosophila* RyR-C (○) and mammalian RyR-C (△) channels. The mean outward and inward conductance values are indicated.

Divalent-cation selectivity of the *Drosophila* RyR-C channel

To further characterize the ion conduction property of the *Drosophila* RyR-C channel, experiments were performed under asymmetrical ionic conditions (Fig. 8). To permit the presence of Ba in the recording solution, the anion gluconate was replaced with methane sulfonate (MES), because $\text{Ba}(\text{gluconate})_2$ is insoluble in H_2O at concentrations larger than 50 mM. Under a Cs concentration gradient of 200 mM (*cis*)/ 50 mM (*trans*), the I-V curve of the *Drosophila* RyR-C channel had a reversal potential of $V_{\text{rev}} \approx -15$

mV, suggesting the cation-selective feature of the *Drosophila* RyR-C channel (Fig. 8 C). Upon the addition of 100 mM $\text{Ba}(\text{MES})_2$ to the *trans* solution, both inward and outward currents decreased. The reversal potential was shifted to the positive direction ($V_{\text{rev}} \approx +17$ mV) (Fig. 8 C), suggesting that the *Drosophila* RyR-C channel is selective for Ba over Cs ions. Thus the *Drosophila* RyR-C channel, like to the mammalian RyR channels, is selective for divalent cations.

DISCUSSION

In this study we have cloned the entire cDNA sequence encoding the *Drosophila* ryanodine receptor, using RT-PCR and cDNA library screening strategies. The Ca^{2+} release channel function of the cloned *Drosophila* RyR was examined in transiently transfected CHO cells. The present study focused on functional characterization of a deletion mutant of *Drosophila* RyR, *Drosophila* RyR-C, which retains $\sim 20\%$ of the *Drosophila* RyR protein, consisting mostly of the transmembrane domain at the carboxyl-terminal end. Using confocal microscopic imaging of CHO cells transfected with GFP-*Drosophila* RyR and GFP-*Drosophila* RyR-C fusion constructs, we showed that the *Drosophila* RyR proteins could be expressed in the intracellular membranes of these cells. Using the lipid bilayer reconstitution method, we found that the *Drosophila* RyR-C proteins are capable of forming functional Ca^{2+} release channels that are selective for divalent over monovalent cations. Opening of the *Drosophila* RyR-C channel requires the presence of micromolar concentrations of Ca^{2+} in the cytosolic solution, but the channel is insensitive to inactivation by millimolar concentrations of Ca^{2+} . These results are similar to those of our previous studies of the carboxyl-terminal portion of the rabbit skeletal muscle Ca^{2+} release channel, RyR-C (Bhat et al., 1997b). Taken together, our data are consistent with the current concept that the putative conduction pore of the Ca^{2+} release channel is located at the carboxyl-terminal portion of the RyR protein.

The level of protein expression with the full-length *Drosophila* RyR is low and transient in the CHO cells, which prevents us from detailed functional characterization of the full-length *Drosophila* RyR channel. In our previous studies with the skeletal and cardiac RyRs from rabbit muscle, we were able to generate stable clones of CHO cells permanently expressing the full-length RyR proteins and their various mutants (Bhat et al., 1997b, 1999). Therefore, the difficulty with the *Drosophila* RyR expression is likely due to the toxic effect of *Drosophila* RyR on CHO cells. The primary amino acid sequence of *Drosophila* RyR is only $\sim 45\%$ homologous to those of the mammalian isoforms of RyRs, and the regions of divergence between the insect and mammalian RyRs may be responsible for the potential toxic effect of the insect Ca^{2+} release channels on CHO cells.

Our preliminary study with the full-length *Drosophila* RyR channel was carried out with transient expression in

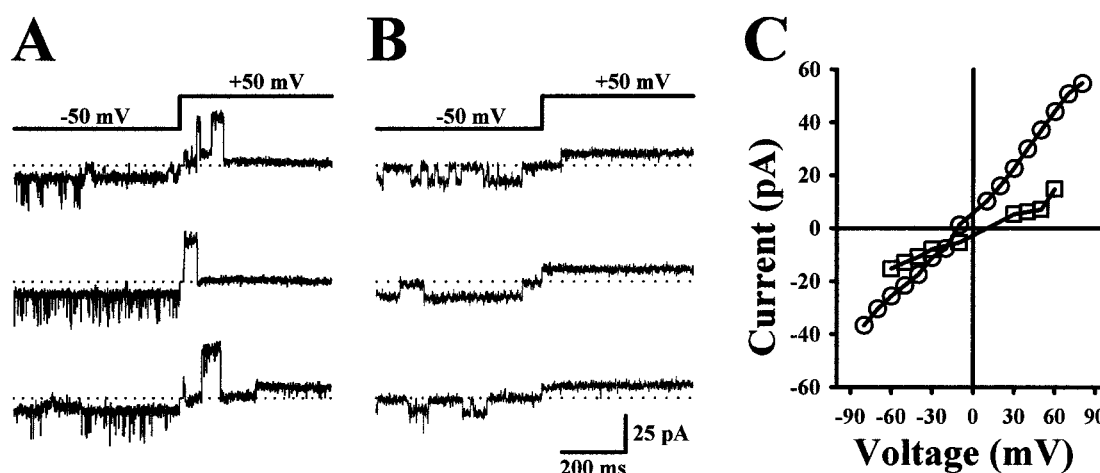


FIGURE 8 Recording of a *Drosophila* RyR-C channel under asymmetrical ionic conditions: selected current traces through the *Drosophila* RyR-C channel under a Cs concentration gradient of 200 mM Cs-methane sulfonate (*cis*)/50 mM (*trans*) (A), and after addition of 100 mM Ba (methane sulfonate)₂ to the *trans* solution (B). (C) The corresponding current-voltage relationship of *Drosophila* RyR-C channel. ○, Currents under 200/50 mM Cs-methane sulfonate; □, currents after the addition of 100 mM Ba(methanesulfonate)₂ to *trans* solution.

CHO cells (Fig. 4). To circumvent the problem with the lack of specific antibodies against *Drosophila* RyR, we have generated GFP-*Drosophila* RyR and GFP-*Drosophila* RyR-C fusion proteins. With antibody against GFP, both GFP-*Drosophila* RyR-C and GFP-*Drosophila* RyR proteins could be detected on the Western blot, although the level of GFP-*Drosophila* RyR was significantly lower than GFP-*Drosophila* RyR-C (Fig. 3 B). We are currently in the process of generating a monoclonal antibody that is specific for the *Drosophila* RyR protein, to quantify the amount of *Drosophila* RyR proteins expressed in the heterologous cell systems. The availability of such a specific antibody will also enable us to develop stable cell lines permanently expressing the *Drosophila* RyR proteins. The successful expression of *Drosophila* RyR in situ will provide a helpful tool for understanding the toxicological mechanism of ryanodine and its derivatives in insect muscle, brain, and other tissues.

Compared with the RyR channels from mammalian cells, the *Drosophila* RyR channel exhibits different conductance properties. For example, the conductance state of the *Drosophila* RyR-C channel is significantly larger than that of the mammalian RyR-C channel (Fig. 5), and furthermore, the *Drosophila* RyR-C channel exhibits frequent transitions to subconductance states. Ryanodine reduced the conductance of the *Drosophila* RyR-C to ~30% of the full conductance state (Fig. 5 C). This is significantly different from the effect of ryanodine on the mammalian RyR channels, where a ~50% reduction in single-channel conductance was observed with both the full-length RyR1 and RyR1-C channels (Bhat et al., 1997b) and with the full-length RyR2 channel (Bhat et al., 1999). It is possible that the use of higher concentrations of ryanodine (40 μ M with *Drosophila* RyR-C versus 5 μ M with mammalian RyR1-C) may lead to

reduction of the single-channel conductance, as had been observed in the studies of Tinker et al. (1996). Alternatively, the conductance state observed in Fig. 5 C actually represents one of the subconductance states associated with the ryanodine-modified channels. The RyR channel from rabbit skeletal muscle also has been shown to exhibit multiple subconductance states when modified by ryanodine (Ma, 1993). It is also possible that the lower conductance state of the ryanodine-modified *Drosophila* RyR-C channel represents a structural difference between the mammalian and insect RyR proteins. These differences could reflect the differences in the primary structure between the mammalian and insect RyRs or be due to interaction with accessory proteins (Brillantes et al., 1994; Qi et al., 1998). It will be important to know how these accessory proteins, such as FKBP12, interact differentially with the mammalian and insect RyRs and contribute to the overall conduction properties and gating kinetics of the Ca release channels. It is interesting that both mammalian RyR-C and *Drosophila* RyR-C channels exhibit rectification in their *I-V* relationship, which suggests the role of the cytoplasmic domain of RyR in the Ca²⁺ release channel function (Bhat et al., 1997a,b). With the use of a ligand binding assay, it has been well established that the binding site for ryanodine is located within the transmembrane domain of the RyR protein from mammalian cells (Witcher et al., 1994; Callaway et al., 1994). It is also known that the cytoplasmic domain of RyR contributes to the high-affinity binding of ryanodine, because the truncated RyR exhibits only low-affinity binding to ryanodine (Ma and Valdivia, unpublished observation).

The primary amino acid sequence of the *Drosophila* RyR shares only 45% homology with the mammalian isoforms of RyRs. There are regions of high divergence between the mammalian and insect isoforms of RyRs, which could serve

as potential targets for the potent insecticides that interact specifically with the insect but not the mammalian isoforms of RyR. These regions are located mostly in the cytoplasmic domains (such as a.a. 1, 167–1, 199, etc). The availability of the cDNA for *Drosophila* RyR opens a new avenue for future structure-function studies with the insect RyR/Ca²⁺ release channels. It will be interesting to know the role the high-divergence region(s) play in the function of the insect RyR channels.

This work was supported by a National Institutes of Health grant (R01-AG15556) and an Established Investigatorship from the American Heart Association to JM, a postdoctoral fellowship from the American Heart Association (NorthEast Ohio Affiliate) to MBB, and a gift from the FMC Corp.

REFERENCES

- Bhat, M. B., S. M. Hayek, J. Zhao, W. Zang, H. Takeshima, W. G. Wier, and J. Ma. 1999. Expression and functional characterization of cardiac ryanodine receptor calcium release channel in Chinese hamster ovary cells. *Biophys. J.* 77:808–816.
- Bhat, M. B., J. Y. Zhao, S. M. Hayek, E. C. Freeman, H. Takeshima, and J. Ma. 1997a. Deletion of amino acids 1641–2437 from the foot region of skeletal muscle ryanodine receptor alters the conduction properties of the calcium release channel. *Biophys. J.* 73:1320–1328.
- Bhat, M. B., J. Y. Zhao, H. Takeshima, and J. Ma. 1997b. Functional Ca²⁺ release channel formed by the carboxyl-terminal portion of ryanodine receptor. *Biophys. J.* 73:1329–1336.
- Bhat, M. B., J. Y. Zhao, W. Zang, C. W. Balke, H. Takeshima, W. G. Wier, and Ma, J. 1997c. Caffeine-induced release of intracellular Ca²⁺ from Chinese hamster ovary cells expressing skeletal muscle ryanodine receptor. *J. Gen. Physiol.* 110:749–762.
- Bidasee, K. R., and H. R. Besch, Jr. 1998. Structure-function relationships among ryanodine derivatives. Pyridyl ryanodine definitively separates activation potency from high affinity. *J. Biol. Chem.* 273:12176–12186.
- Brillantes, A. B., K. Ondrias, A. Scott, E. Kobrinisky, E. Ondriasova, M. C. Moschella, T. Jayaraman, M. Landers, B. E. Ehrlich, and A. R. Marks. 1994. Stabilization of calcium release channel/ryanodine receptor function by FK506-binding protein. *Cell.* 77:513–523.
- Callaway, C., A. Seryshev, J. P. Wang, K. J. Slavik, D. H. Needleman, C. Cantu, Y. Wu, T. Jayaraman, A. R. Marks, and S. L. Hamilton. 1994. Localization of the high and low affinity [³H]-ryanodine binding sites on the skeletal muscle Ca²⁺ release channel. *J. Biol. Chem.* 269:15876–15884.
- Du, G. G., J. P. Imredy, and D. H. MacLennan. 1998. Characterization of recombinant rabbit cardiac and skeletal muscle Ca²⁺ release channels (ryanodine receptors) with a novel [³H]ryanodine binding assay. *J. Biol. Chem.* 273:33259–33266.
- Fleischer, S., and M. Inui. 1989. Biochemistry and biophysics of excitation-contraction coupling. *Annu. Rev. Biophys. Chem.* 18:333–364.
- Gao, L., A. Tripathy, X. Lu, and G. Meissner. 1997. Evidence for a role of C-terminal amino acid residues in skeletal muscle Ca²⁺ release channel (ryanodine receptor) function. *FEBS Lett.* 412:223–226.
- Hakamata, Y., J. Nakai, H. Takeshima, and K. Imoto. 1992. Primary structure and distribution of a novel ryanodine receptor/calcium release from rabbit brain. *FEBS Lett.* 312:229–235.
- Hasan, G., and M. Rosbash. 1992. *Drosophila* homologs of two mammalian intracellular Ca²⁺ release channels: identification and expression patterns of the inositol 1,4,5-trisphosphate and the ryanodine receptor genes. *Development.* 116:967–975.
- Jenden, D. J., and A. S. Fairhurst. 1969. The pharmacology of ryanodine. *Pharmacol. Rev.* 21:1–25.
- Ma, J. 1993. Block by ruthenium red of the ryanodine-activated calcium release channel of skeletal muscle. *J. Gen. Physiol.* 102:1031–1056.
- Ma, J., and J. Y. Zhao. 1994. Highly cooperative and hysteretic response of the skeletal muscle ryanodine receptor to changes in proton concentrations. *Biophys. J.* 67:626–633.
- McPherson, P. S., and K. P. Campbell. 1993. The ryanodine receptor/Ca²⁺ release channel. *J. Biol. Chem.* 268:13765–13768.
- Meissner, G. 1984. Adenine nucleotide stimulation of Ca²⁺-induced Ca²⁺ release in sarcoplasmic reticulum. *J. Biol. Chem.* 259:2365–2374.
- Otsu, K., H. F. Willard, V. K. Khanna, F. Zorzato, N. M. Green, and D. H. MacLennan. 1990. Molecular cloning of cDNA encoding the Ca²⁺ release channel (ryanodine receptor) of rabbit cardiac muscle sarcoplasmic reticulum. *J. Biol. Chem.* 265:13472–13483.
- Pepper, B. P., and L. A. Carruth. 1945. A new plant insecticide for control of the European corn borer. *J. Econ. Entomol.* 38:59–66.
- Qi, Y., M. Ogunbunmi, E. A. Freund, A. P. Timerman, and S. Fleischer. 1998. FK-binding protein is associated with the ryanodine receptor of skeletal muscle in vertebrate animals. *J. Biol. Chem.* 273:34813–34819.
- Schmitt, M., A. Turberg, and M. Londershausen. 1997. Characterization of a ryanodine receptor in *Periplaneta americana*. *J. Recept. Signal Transduction Res.* 17:185–197.
- Sutko, J. L., and J. A. Airey. 1996. Ryanodine receptor Ca²⁺ release channels: does diversity in form equal diversity in function? *Physiol. Rev.* 76:1027–1071.
- Takeshima, H. 1993. Primary structure and expression from cDNAs of the ryanodine receptor. *Ann. N.Y. Acad. Sci.* 707:165–177.
- Takeshima, H., M. Nishi, N. Iwabe, T. Miyata, T. Hosoya, I. Masai, and Y. Hotta. 1994. Isolation and characterization of a gene for a ryanodine receptor/calcium release channel in *Drosophila melanogaster*. *FEBS Lett.* 337:81–87.
- Takeshima, H., S. Nishimura, T. Matsumoto, H. Ishida, K. Kangawa, N. Minamino, H. Matsuo, M. Ueda, M. Hanaoka, T. Hirose, and S. Numa. 1989. Primary structure and expression from complementary DNA of skeletal muscle ryanodine receptor. *Nature.* 339:439–445.
- Tinker, A., J. L. Sutko, L. Ruest, P. Deslongchamps, W. Welch, J. A. Airey, K. Gerzon, K. R. Bidasee, H. R. Besch, Jr., and A. J. Williams. 1996. Electrophysiological effects of ryanodine derivatives on the sheep cardiac sarcoplasmic reticulum calcium-release channel. *Biophys. J.* 70:2110–2119.
- Usherwood, P. N., and H. Vais. 1995. Towards the development of ryanoid insecticides with low mammalian toxicity. *Toxicol. Lett.* 82–83:247–254.
- Wagenknecht, T., R. Grassucci, J. Frank, A. Saito, M. Inui, and S. Fleischer. 1989. Three dimensional architecture of the calcium channel/foot structure of sarcoplasmic reticulum. *Nature.* 338:167–170.
- Waterhouse, A. L., I. N. Pessah, A. Q. Francini, and J. E. Casida. 1987. Structural aspects of ryanodine action and selectivity. *J. Med. Chem.* 30:710–716.
- Wayne Chen, S. R., P. Leong, J. P. Imredy, C. Bartlett, L. Zhang, and D. H. MacLennan. 1997. Single-channel properties of the recombinant skeletal muscle Ca release channel (ryanodine receptor). *Biophys. J.* 73:1904–1912.
- Welch, W., J. L. Sutko, K. E. Mitchell, J. A. Airey, and L. Ruest. 1996. The pyrrrol locus is the major orienting factor in ryanodine binding. *Biochemistry.* 35:7165–7173.
- Welch, W., A. J. Williams, A. Tinker, K. E. Mitchell, P. Deslongchamps, J. Lamothe, K. Gerzon, K. R. Bidasee, H. R. Besch, Jr., J. A. Airey, J. L. Sutko, and L. Ruest. 1997. Structural components of ryanodine responsible for modulation of sarcoplasmic reticulum calcium channel function. *Biochemistry.* 36:2939–2950.
- Witcher, D. R., P. S. McPherson, S. D. Kahl, T. Lewis, P. Bentley, M. J. Mullinix, J. D. Windass, and K. P. Campbell. 1994. Photoaffinity labeling of the ryanodine receptor/Ca²⁺ release channel with an azido derivative of ryanodine. *J. Biol. Chem.* 269:13076–13079.